

Corrosion Protection of 304 Stainless Steel Bipolar Plates of PEMFC by Coating SnO₂ Film

Linghui Yang, Zhenlan Qin, Hongtao Pan, Hong Yun*, Yulin Min and Qunjie Xu*

Shanghai Key Laboratory of Materials Protection and Advanced Materials in Electric Power, Shanghai Engineering Research Center of Energy-Saving in Heat Exchange Systems, Shanghai University of Electric Power, 2588 Changyang Road, Yangpu District, Shanghai 200090, China

*E-mail: yunhong@shiep.edu.cn; xuqunjie@shiep.edu.cn

Received: 28 June 2017 / *Accepted:* 16 September 2017 / *Published:* 12 October 2017

Tin oxide (SnO₂) film was successfully coated on surface of austenite 304 stainless steels (304SS) by combining sol-gel dip-coating method with alcohol thermal method. The coated SnO₂ film was used to enhance corrosion resistance of 304SS bipolar plates in a simulated proton exchange membrane fuel cell (PEMFC) environment. Bared 304SS and SnO₂ coated 304SS were investigated via EIS, potentiodynamic polarization curves and potentiostatic polarization curves measurements in a simulated PEMFC cathodic, anodic environment, respectively. Compared with the bared 304SS, the corrosion current density for the SnO₂ coated 304SS was decreased significantly from 33.22 μA/cm² to 0.1327 μA/cm² in a simulated cathodic environment, and from 75.079 μA/cm² to 0.1581 μA/cm² in a simulated anodic environment. Surface structure and chemical composition of the samples were obtained by SEM, EDX, AFM, XRD and XPS. The result showed that a uniform and compact SnO₂ film was coated on the surface of 304SS, which enhanced the corrosion resistance of 304SS in a simulated PEMFC environment.

Keywords: Proton exchange membrane fuel cell (PEMFC); 304 stainless steel; bipolar plate; tin oxide (SnO₂) film; corrosion

1. INTRODUCTION

Proton exchange membrane fuel cell (PEMFC) is a clean energy system for conversing elementary energy of H₂ and O₂ into electric power. It is environmentally friendly, long life, easy start-up at low temperatures and offers high energy efficiency and high specific power. It is not only with a good potential for use in military and portable instruments, but also suitable for mobile power supplies. Therefore, PEMFC is an ideal candidate for the optimal home power system [1-3].

The bipolar plate, a multi-functional component, is one of the key elements in PEMFC system. It is used to collect the current, distribute fuel and oxygen, separate individual cells, and facilitate water and heat management [4]. The performance quality of the bipolar plate directly affects the output power and service life of the battery. Stainless steel is one of the most prospective bipolar plate materials because of its good chemical stability, high strength and low cost. However, corrosion and passivation of stainless steel bipolar plates in PEMFC environments is a long-study problem [5-12]. Thus, coating process has been adopted to protect the stainless steel bipolar plates. At present, a lot of methods, such as chemical vapor deposition (CVD) [13], electrodeposition method [8], arc ion plating [11] and ion sputtering [14, 15], have been developed for surface modification of stainless steel bipolar plates.

Among them, CVD could prepare highly oriented nano-array, but went against large area preparation because of harsh conditions and complicated operation. Electrodeposition needs a high requirement of substrate, and easily forms some pinhole pore. Arc ion plating and ion sputtering operates complex and limited application. Compared with CVD method, electrodeposition method, arc ion plating and ion sputtering, hydrothermal method and alcohol thermal method have many advantages, such as mild reaction conditions, no pollution, large-scale synthesis, low production cost and simple operation and etc. It is an effective method for producing large-scale nano-array materials. Zhao [16] fabricated a porous TiO_2 film onto the stainless steel plates via sol-gel dip-coating method and hydrothermal method. Qin [17] successfully synthesized nanostructure ZSM-5 zeolite with the TPABr and TPAOH as the templates by hydrothermal synthesis. Compared with conventional hydrothermal method, alcohol thermal method can accurately control the reaction rate of precursor and form uniform films with some morphology and crystalline structure. It has ample reaction time to precursor, and be helpful to assembly and aggregation. Currently, the application of alcohol thermal method on preparation of nano-wires, nano-rods, nano-particles have been studied deeply, but few researches carry out on thin film by alcohol thermal method. Zhang [18] prepared Cadmium Selenide nanocrystals/thin films on the substrate by using alcohol thermal method, which was well applied in solar cell devices with a high efficiency. You [19] successfully synthesized pentagonal silver nano-wires with diameters in range of 20~40 nm, and lengths up to $\sim 10\mu\text{m}$ via alcohol-thermal route.

There have been a lot of reports about the oxide films [20, 21] to modify the surface of different material. Miao [22] applied a spray pyrolysis technique to deposit thin films of SnO_2 : F onto preheated glass substrates by using dihydrate stannous chloride ($\text{SnCl}_2 \cdot 2\text{H}_2\text{O}$) and ammonium fluoride (NH_4F) as the precursors. Inoue [23] used a polygonal barrel sputtering system to modify the surface of Al_2O_3 particles with Au. However, because of the excellent corrosion resistance and metal-like conductivity, SnO_2 film could be used for corrosion protection and even used as a potential candidate to protect bipolar plate from corrosion in PEMFC. Wang [24, 25] found that SnO_2 : F coated some ferritic stainless steels and austenite stainless steels in simulated PEMFC environments exhibited a good corrosion resistance.

In this paper, SnO_2 film was coated on 304SS sample by using a combining method of sol-gel dip-coating and alcohol thermal. The anti-corrosion performance, surface structure and chemical composition of the SnO_2 coated 304SS were investigated as well.

2. EXPERIMENTAL

2.1 Preparation of SnO₂ film

2.1.1 Experiment material

The substrates with dimensions of about 10mm×70mm×2mm were fabricated from a commercial 304SS plate. SnCl₂•2H₂O, PEG2000, KCl, KNO₃, HF, H₂SO₄ and ethanol were purchased from the Sinopharm Chemical Reagent Co, Ltd.(SCRC). All chemicals were used as received without further purification.

2.1.2 Preparation

SnCl₂•2H₂O, ethanol and PEG2000 were selected as starting materials. After 6.4 g SnCl₂•2H₂O was added into a 100ml ethanol solution with 0.46 g PEG2000, the solution was homogenized with a magnetic stirrer at 50 °C for 2 h, and then aged for 24 h. The 304SS (the composition was given in Table 1) substrates were polished step by step with W20~W5 metallographic abrasive papers and thoroughly degreased with ethanol by using an ultrasonic cleaner, and then were rinsed with distilled water.

Table 1. Chemical composition of 304 stainless steel (wt %)

| Element | C | Si | Mn | P | S | Cr | Ni | Fe |
|-----------------|-------|------|------|-------|-------|-------|------|--------|
| Content (wt%) | 0.035 | 0.51 | 1.18 | 0.035 | 0.029 | 17.58 | 8.01 | 71.721 |

The 304SS substrate was dipped into the solution, withdrew at 2 mm/s and dried at room temperature, before it was baked in an oven at 100 °C for 0.5 h. For obtaining the thicker SnO₂ film, the above steps were repeated several times. In a typical alcohol thermal route, the SnO₂ coated 304SS substrates were reacted with the precursor sol solution in a Teflon sealed stainless steel autoclave with an 75% filling factor. The autoclave was put into an oven, heated to 180 °C for 3 h, and cooled naturally in air. Subsequently, the as-deposited substrates were rinsed repeatedly with deionized water and dried in an oven at 100 °C for 0.5 h for further characterization.

2.2. Characterization methods

2.2.1 Electrochemical measurements

A conventional three-electrode system, with a platinum sheet as the counter-electrode and a saturated calomel electrode (SCE) as the reference electrode, was used for the electrochemical measurements. The corrosion tests of 304SS samples with a working surface area of 1 cm² were conducted with a Princeton Applied Research (PAR) 273 potentiostat/ Galvanostat in PEMFC environment (0.05 M H₂SO₄ solution with 2 ppm HF solution) at 70 °C. Potentiodynamic polarization

was undertaken from -0.25 V (SCE) OCP to 1.0 V (SCE) OCP at a scan rate of 1 mV/s. Electrochemical Impedance Spectroscopy (EIS) were made in the range 100 kHz-0.05 Hz, with an amplitude of 5mV for the input sine wave voltage. Potentiostatic current-time curves measurements were carried out in the simulated PEMFC cathodic (0.6 V, air bubbled, 70 °C) and anodic (-0.1 V, H₂ bubbled, 70 °C) environment, respectively.

2.2.2 Surface morphology and chemical composition testing

Surface morphologies of the bared 304SS and SnO₂ film modified 304SS were observed by SEM (Hitachi SU-1500) equipped with an energy dispersive X-ray spectrometer (EDX) and AFM. AFM tip in tapping mode (Molecular Imaging Pico Scan 2100) was also performed on the surfaces of samples. X-ray diffraction (XRD) patterns were obtained using a Bruker D8 Advance diffractometer using a Cu K α source ($k = 0.154056$ nm) at 40 kV and 40 mA. The X-ray photoelectron spectra of the films were obtained by X-ray photoelectron spectrometer (XPS, PHI-5000C ESCA system) with Al K α radiation ($h\nu = 1486.6$ eV). The binding energy was corrected by taking the C1s level as 284.6 eV.

3. RESULTS AND DISCUSSION

3.1 Electrochemical impedance spectroscopy (EIS) and polarization curve tests

To better simulate PEMFC environment, electrochemical tests of the samples were performed at shutting down (room temperature) and working state (70 °C).

3.1.1 Electrochemical tests at shutting down

EIS and polarization tests were carried out to investigate the behavior of bare 304SS and SnO₂ film modified 304SS in 0.05 M H₂SO₄ solution with 2ppm HF at room temperature. Fig. 1 shows the EIS data of bare 304SS and SnO₂ film modified 304SS. It is notable that the Nyquist plots for the SnO₂ film modified 304SS is composed of a large semi-circle, and it's the electrochemical impedance value is significantly higher than that of the bared 304SS. The modified 304SS exhibit high stability in the test solution. It is an effective barrier to the inward penetration, and thus significantly reduces the corrosion of the substrate alloy [26-28].

Fig. 2 illustrates the polarization curves of bare 304SS and SnO₂ film modified 304SS. The self-corrosion potential of the SnO₂ film modified 304SS moved towards the positive direction by 525 mV when compared with that of bare 304SS (Fig. 2 and Table 2). Furthermore, cathodic Tafel slopes (β_c), which were shown in Table 2, could also be obtained by extrapolating the linear portions of the anodic and cathodic branches to their intersections. The corrosion current density decreased from 6.204 $\mu\text{A}/\text{cm}^2$ for the bare 304SS to 0.05065 $\mu\text{A}/\text{cm}^2$ for the SnO₂ film modified 304SS, decreased by about 2~3 orders of magnitude. These results indicated that the SnO₂ film modified 304SS displayed better barrier properties in PEMFC environment. Besides, the film was quite stable during the

polarization, as evidenced by the absence of the current density fluctuation, suggesting no degradation was observed after potentiostatic measurement. In other words, the SnO₂ film was very stable in the simulated PEMFC environment [25-28].

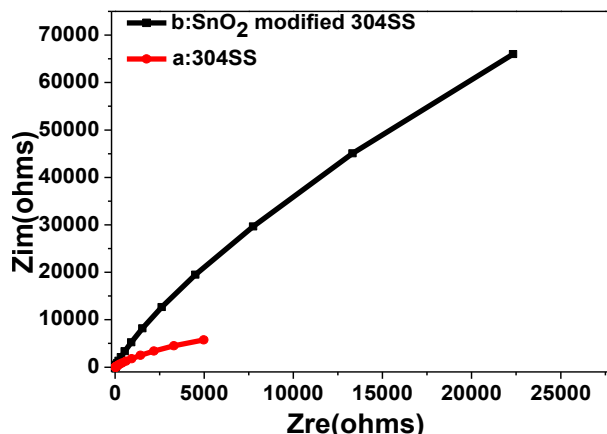


Figure 1. Nyquist plots of the samples in simulated PEMFC environment at shutting down (0.05 M H₂SO₄ + 2 ppm F⁻) (a) 304SS, (b) SnO₂ modified 304SS

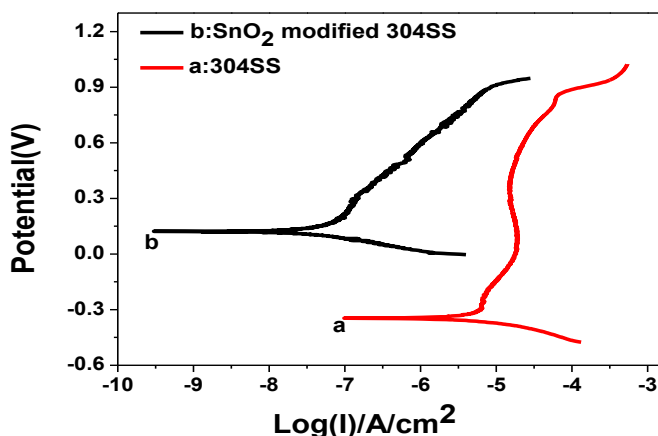


Figure 2. Potentiodynamic polarization curves of the samples in simulated PEMFC environment at stoppage.

Table 2. The corrosion current density (I_{corr}), the corrosion potentials (E_{corr}) and the cathodic Tafel slopes (β_c) values for the samples in simulated PEMFC environment at stoppage

| Sample | E_{corr} (mV) (SCE) | β_c (mV·dec ⁻¹) | I_{corr} (μA/cm ²) |
|----------------|-----------------------|-----------------------------------|----------------------------------|
| Bare 304SS | -345.864 | -249 | 6.204 |
| Modified 304SS | 120.08 | -196 | 0.05065 |

3.1.2 Electrochemical tests at working state

Fig. 3 shows the EIS of bare 304SS and SnO₂ film modified 304SS in 0.05 M H₂SO₄ solution with 2 ppm HF at 70 °C. The EIS were all semicircular and the chord was the symbol of resistance of film (R_f), the corrosion resisting properties increase as R_f increases [25-28]. As shown in Fig. 3, the

corresponding chord of the EIS of SnO₂ film modified 304SS was significantly longer than that of bare 304SS in both simulated PEMFC anodic and cathodic environment, but the impedance values of bare 304SS and SnO₂ film modified 304SS were bigger in simulated cathodic environment. Compared with the EIS results of samples that performed at shutting down, the impedance values of samples at working state decrease a little. This result indicates that the SnO₂ film modified 304SS was an effective barrier to the inward penetration in test solution and had relatively better corrosion resistance.

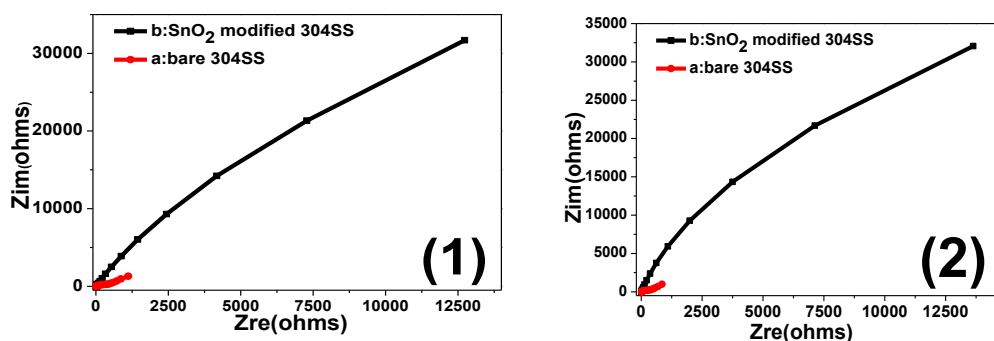


Figure 3. Nyquist plots of the sample a, b in (1) simulated PEMFC cathodic environment (0.05 M H₂SO₄ with 2 ppm HF solution, bubbled with compressed air, 70 °C) and (2) simulated anodic environment (0.05 M H₂SO₄ with 2 ppm HF solution, bubbled with H₂, 70 °C)

The potentiodynamic polarization curves of bare 304SS and SnO₂ film modified 304SS were displayed in Fig. 4. The polarization behavior of the bare 304SS was similar in the simulated PEMFC anodic and cathodic environment. The bare 304SS passivated spontaneously in PEMFC environment, where it was in active state at E_{corr} in anodic environment, but the active region was very narrow [29]. However, some subtle differences between these two curves were observable. The bare 304SS exhibited a self-corrosion potential (E_{corr}) of -330.221 mV vs SCE in the cathodic environment and a corrosion potential of -359.761 mV vs SCE in the anodic environment (Table 3), indicating that a stable passive film is easier to be established in the simulated PEMFC cathodic environment. Fig. 4(a) shows the potentiodynamic polarization results when the solution was bubbled with compressed air to simulate the PEMFC cathodic environment at 70 °C. The current density of 304SS and the SnO₂ film modified 304SS was measured to be 33.22 $\mu\text{A}\cdot\text{cm}^{-2}$ and 0.1327 $\mu\text{A}\cdot\text{cm}^{-2}$, respectively, in the cathodic environment. The SnO₂ film modified 304SS showed a 2~3 orders of magnitude decreased current density compared with that of bare 304SS.

Fig. 4(b) shows the potentiodynamic polarization results in the simulated anodic environment (bubbled with compressed air). Comparing with the curves, the self-corrosion potential of 304SS was -359.761 mV vs SCE, whereas the SnO₂ film modified 304SS had a more positive E_{corr} , 117.373 mV (Table 3). Also, the results of cathodic Tafel slopes (β_c) were shown in Table 3. The current density of 304SS in the anodic environment was 75.079 $\mu\text{A}/\text{cm}^2$, whereas the SnO₂ film modified 304SS was 0.1581 $\mu\text{A}/\text{cm}^2$. The current density of SnO₂ film modified 304SS decreased by about 2~3 orders of magnitude compared to that of bare 304SS. Besides, the SnO₂ film was quite stable during the polarization, as evidenced by the absence of the current density fluctuation, suggesting no degradation

was observed after potentiostatic measurement and indicating the SnO₂ film is very stable in simulated PEMFC (bubbled with H₂). The bare 304SS showed a somewhat different performance from that of SnO₂ film modified 304SS. As for the experiments in 0.05 M H₂SO₄ + 2 ppm HF solution at 70 °C (in simulated PEMFC working state environment) bubbled with air (Fig. 4(1)) or H₂ (Fig. 4(2)), the corrosion currents the corrosion currents were higher than that performed at 25 °C. But SnO₂ modified 304SS exhibited a better corrosion resistance than bared 304SS in all simulated PEMFC environments.

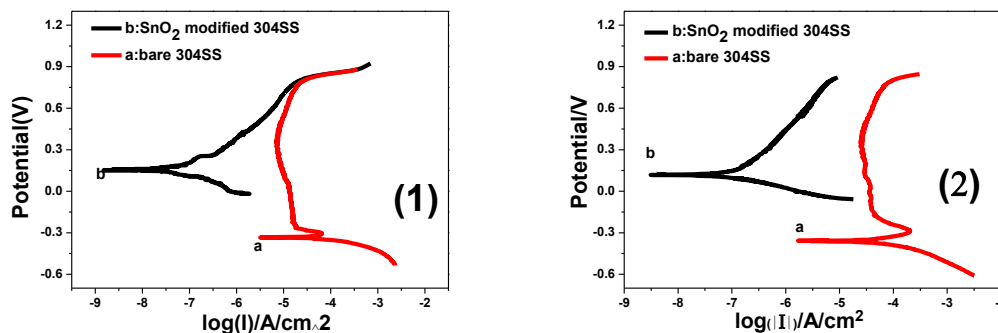


Figure 4. Potentiodynamic polarization curves of the samples a, b in (1) simulated PEMFC cathodic environment and (2) simulated anodic environment.

Table 3. The corrosion current density (I_{corr}), the corrosion potentials (E_{corr}) and the cathodic Tafel slopes (β_c) values for the samples a, b in simulated PEMFC environment

| Sample | | E_{corr} (mV) | β_c | I_{corr} ($\mu\text{A}/\text{cm}^2$) |
|----------------|----------------|-----------------|-------------------------------------|--|
| cathodic | anodic | (SCE) | ($\text{mV}\cdot\text{dec}^{-1}$) | |
| Bare 304SS | — | -330.221 | -254 | 33.22 |
| Modified 304SS | — | 140.651 | -431 | 0.1327 |
| — | Bare 304SS | -359.761 | -473 | 75.079 |
| — | Modified 304SS | 117.373 | -218 | 0.1581 |

3.2 Potentiostatic polarization

Potentiostatic polarization measurements were used to further evaluate the performance of the modified SnO₂ coating 304SS. Fig. 5 shows the potentiostatic polarization curves of the bare 304SS and the SnO₂ film modified 304SS in stimulated cathodic and anodic environment. With a compressed air purge, the polarization current of bare 304SS and SnO₂ film modified 304SS decreased instantly after polarization at 0.6V to the level of $10^{-5.7}$ A/cm² and $10^{-7.1}$ A/cm², respectively, in stimulated cathodic environment. With a hydrogen gas purge, the polarization current of bare 304SS and SnO₂ film modified 304SS decreased instantly after polarization at -0.1 V to the level of 10^{-4} A/cm² and $10^{-5.6}$ A/cm², respectively, in stimulated anodic environment. It shows clearly that the SnO₂ film could effectively inhibit corrosion of the substrate stainless steel in the PEMFC environment [30]. The SnO₂ film modified 304SS is then becoming much more stable than the bare 304SS.

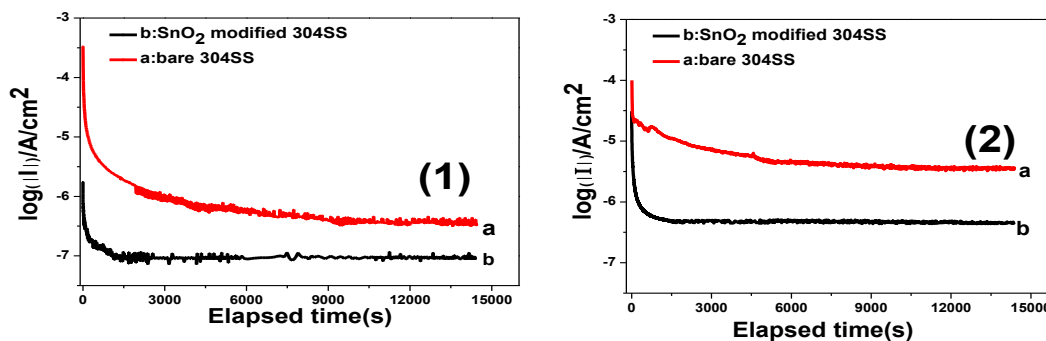


Figure 5. Potentiostatic test for a, b at steady potential in (1) simulated cathodic environment (0.6 V vs SCE bubbled with compressed air, 70 °C) and (2) simulated anodic environment (-0.1 V vs SCE bubbled with H₂, 70 °C)

3.3 Surface morphologies of the SnO₂ film coated 304SS

AFM and SEM measurements were conducted to obtain the qualitative information of the film surface morphology. Fig. 6 shows the AFM images of the SnO₂ film modified and unmodified 304SS samples. It is noted that a thin film was deposited on 304SS, and the thickness of the vertical SnO₂ thin film was in the range of 220-320 nm. The micrograph shows that the film is continuous with a straight distribution with well-covered grains of different sizes averaging to 200-300 nm. This is the probably reason that higher substrate temperatures lead to the formation of larger SnO₂ crystallites, resulting in a rougher surface, which could lead to the enhancement of corrosion resistance [31].

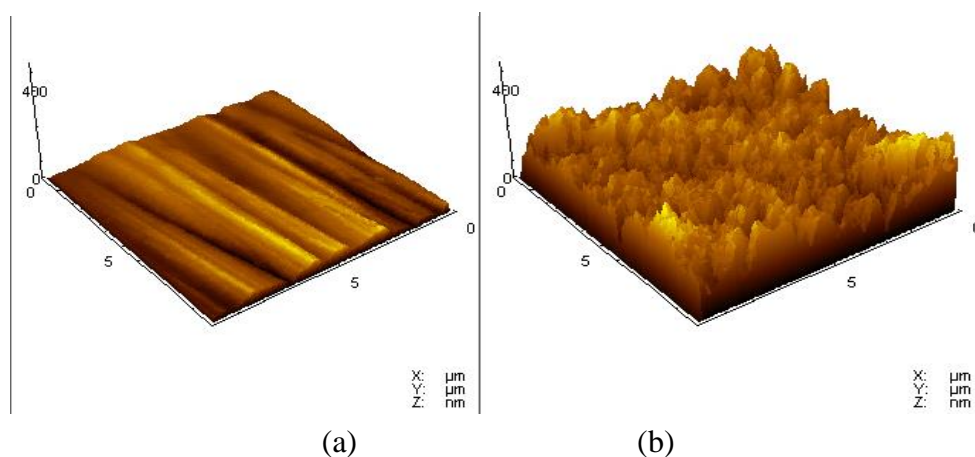


Figure 6. 3D AFM surface images of samples, (a) 304 SS (b) SnO₂ film modified 304SS

SEM/EDS is often used to determine the element distribution in a composite film [32-35]. Fig. 7 shows the SEM image of the SnO₂ film modified 304SS. For comparison, the SEM image of 304SS was also included in the figure. As shown in Fig. 7(b), the prepared SnO₂ thin film demonstrated somewhat micro-structural morphology of the grains.

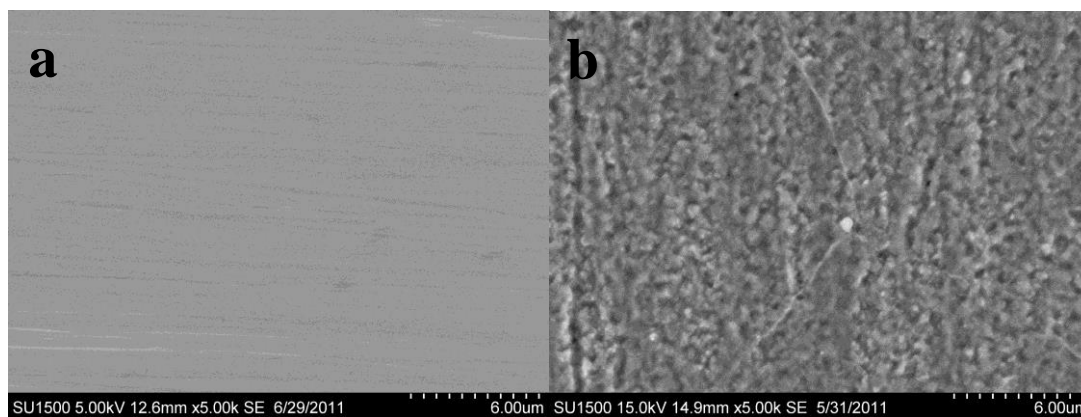


Figure 7. Surface morphology of samples with 5000 amplification (a) bare 304SS, (b) SnO₂ film modified 304SS

3.4 Chemical composition of the SnO₂ film coated 304SS

X-ray diffraction (XRD) is an effective way to study the crystalline structure [36] of SnO₂ film. Fig. 8 shows the XRD patterns of SnO₂ thin film modified 304SS. As shown in the figure, several strong diffraction peaks at 42.2°, 45.7°, 48.1°, which could be attributed to the 304SS substrate, appear on the XRD patterns. A few broad peaks at 26.2°, 34.2°, 52.3° corresponding to the tetragonal rutile phase of SnO₂ [22, 35, 37, 38] are also presented for the modified 304SS. The broad peaks indicate poor crystallinity and small crystallite size of SnO₂ crystals in the film.

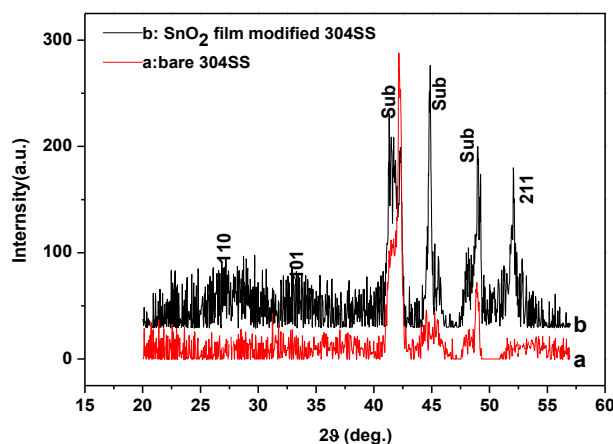


Figure 8. XRD patterns of samples (a) bare 304SS, (b) SnO₂ film modified 304SS

The chemical state and composition for the SnO₂ modified 304SS were measured by XPS analyses. Fig. 9 shows the XPS Sn3d and O1s spectral windows of using combing sol-gel dip-coating method with alcohol thermal method (180 °C, 3 h). The binding energy of Sn 3d electron at 486.8 and 495.4 eV, and the binding energy of O 1s electron at 531.3 eV was observed, which are in good agreement with reported data [39-42]. Moreover, the calculated O: Sn is 2.981, and oxygen content is sufficient in film layer, which suggest that they existed in the forms of SnO₂.

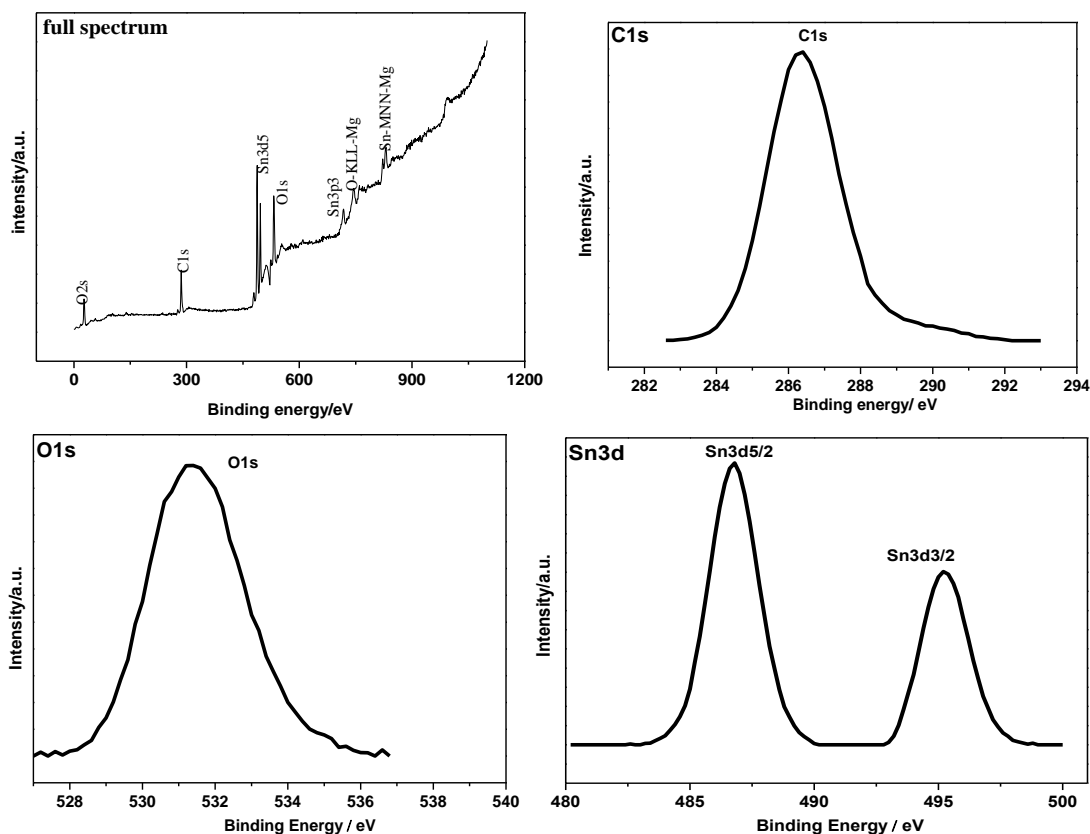


Figure 9. XPS spectra for O1s and Sn3d of SnO₂ film coated 304SS

4. CONCLUSIONS

Austenite 304 stainless steels (304SS) have been coated SnO₂ by combining sol-gel dip-coating method with alcohol thermal method at 180 °C for 3 h and investigated in a simulated proton exchange membrane fuel cell (PEMFC) cathodic and anodic environment, respectively. The electrochemical test results showed that the corrosion resistance of 304SS was significantly improved by SnO₂ surface layer coating. In specific, the corrosion potential (E_{corr}) of SnO₂ film modified 304SS was shifted from -330.22 to 140.651 mV vs SCE in simulated PEMFC cathodic environment and from -359.76 to 117.37 mV vs SCE in simulated PEMFC anodic environment. Corrosion current density decreased significantly from 33.22 $\mu\text{A}/\text{cm}^2$ for the bare 304SS to 0.1327 $\mu\text{A}/\text{cm}^2$ for the SnO₂ coated 304SS in simulated cathodic environment, and from 75.079 $\mu\text{A}/\text{cm}^2$ to 0.1581 $\mu\text{A}/\text{cm}^2$ in simulated anodic environment. After 14400s potentiostatic polarization curves measurements in the simulated PEMFC environment, a sharp current decrease appears for the bare 304SS. In contrast, the sharpest current drop appears for the SnO₂ film modified 304SS, the currents could finally reach an invariable value. The SEM and AFM results indicate that a SnO₂ thin film was deposited on 304SS, and the thickness of the vertical SnO₂ thin film was in the range of 220-320 nm. The XRD results show that SnO₂ film formed on the surface of 304SS was a poor crystallinity. The XPS results obtained from the modified

SnO₂ coating 304SS suggest that Sn existed in the forms of SnO₂. Therefore, it is possible that SnO₂ film modified 304SS could be used as bipolar plates in a PEMFC.

ACKNOWLEDGEMENTS

This work was financially supported by National Natural Science Foundation of China (No. 21673135) and Science and Technology Commission of Shanghai Municipality (No.17020500700).

References

1. A. Arsalis, M. P. Nielsen and S. K. Kær, *Energy*, 36 (2011) 993.
2. L. Barelli, G. Bidini, F. Gallorini and A. Ottaviano, *Appl. Energy*, 91 (2012) 13.
3. Elmer, M. Worall, S. Wu and S. B. Riffat, *Renew. Sust. Energ. Rev.*, 42 (2015) 913.
4. S. Mahabunphachai, Ö. N. Cora and M. Koç, *J. Power Sources*, 195 (2010) 5269.
5. D. Zhang, L. Duan, L. Guo and W. H. Tuan, *Int. J. Hydrogen Energy*, 35 (2010) 3721.
6. Y. Zhao, L. Wei, P. Yi and L. Peng, *Int. J. Hydrogen Energy*, 41 (2016) 1142.
7. L. Wang, J. Sun, B. Kang, S. Li, S. Ji, Z. Wen and X. Wang, *J. Power Sources*, 246 (2014) 775.
8. N. Mohammadi, M. Yari and S. R. Allahkaram, *Surf. Coat. Technol.*, 236 (2013) 341.
9. N. Huang, H. Yu, L. Xu, S. Zhan, M. Sun and D. W. Kirk, *Results in Physics*, 6 (2016) 730.
10. A. S. Gago, S. A. Ansar, B. Saruhan, U. Schulz, P. Lettenmeier, N. A. Cañas, P. Gazdzicki, T. Morawietz, R. Hiesgen, J. Arnold and K. A. Friedrich, *J. Power Sources*, 307 (2016) 815.
11. M. Zhang, G. Lin, B. Wu and Z. Shao, *J. Power Sources*, 205 (2012) 318.
12. K. Huang, D. Zhang, M. Hu and Q. Hu, *Energy*, 76 (2014) 816.
13. M. Hashempour, A. Vicenzo, F. Zhao and M. Bestetti, *Mater. Charact.*, 92 (2014) 64.
14. P. Yi, L. Peng, L. Feng, P. Gan, and X. Lai, *J. Power Sources*, 195 (2010) 7061.
15. L. Wang, J. Sun, J. Sun, Y. Lv, S. Li, S. Ji and Z. Wen, *J. Power Sources*, 199 (2012) 195.
16. X. Zhao, M. Liu and Y. Zhu, *Thin Solid Films*, 515 (2007) 7127.
17. R. Karimi, B. Bayati, N. C. Aghdam, M. Ejtemaee and A. A. Babaluo, *Powder technol.*, 229 (2012) 229.
18. Y. Zhang, P. Li, W. M. Lau, Y. Gao, J. Zi and Z. Zheng, *Mater. Chem. Phys.*, 145 (2014) 441.
19. T. You, S. Xu, S. Sun and X. Song, *Mater. Lett.*, 63 (2009) 920.
20. W. Liu, Q. Xu, J. Han, X. Chen and Y. Min, *Corros. Sci.*, 110 (2016) 105.
21. H. Jie, Q. Xu, L. Wei and Y. Min, *Corros. Sci.*, 102 (2016) 251.
22. D. Miao, Q. Zhao, S. Wu, Z. Wang, X. Zhang and X. Zhao, *J. Non-Cryst. Solids*, 356 (2010) 2557.
23. M. Inoue, Y. Takahashi, M. Katagiri, T. Abe and M. Umeda, *J. Alloys Compd.*, 670 (2016) 170.
24. H. Wang and J. A. Turner, *J. Power Sources*, 170 (2007) 387.
25. H. Wang, J. A. Turner, X. Li and G. Teeter, *Power Sources*, 178 (2008) 238.
26. L. Cui, R. Zeng, S. Li, F. Zhang and E. H. Han, *RSC Adv.*, 6 (2016) 63107.
27. H. Sun, X. Wu and E. Han, *Corros. Sci.*, 51 (2009) 2840.
28. M. O. Oteyaka and H. Ayrature, *Int. J. Electrochem. Sci.*, 10 (2015) 8549.
29. C. Li, Y. Ma, Y. Li and F. Wang, *Corros. Sci.*, 53 (2011) 2549.
30. W. Liu, W. Cao, X. Deng, Y. Min and Q. Xu, *Int. J. Electrochem. Sci.*, 10 (2015) 8858.
31. M. Li, Q. Xu, J. Han, H. Yun and Y. Min, *Int. J. Electrochem. Sci.*, 10 (2015) 9028.
32. X. Jin, Q. Xu, H. Liu, X. Yuan and Y. Xia, *Electrochim. Acta*, 136 (2014) 19.
33. ³³Y. Min, G. He, Q. Xu and Y. Chen, *J. Mater. Chem. A*, 2 (2014) 2578.
34. T. Wang, J. He, D. Sun, J. Zhou, Y. Guo, X. Ding, S. Wu, J. Zhao and J. Tang, *Corros. Sci.*, 53 (2011) 1498.
35. L. Zhang, Y. Zhong, D. Cha and P. Wang, *Sci. Rep.*, 3 (2013).

36. X. Jin, Q. Xu, X. Yuan, L. Zhou and Y. Xia, *Electrochim. Acta*, 114 (2013) 605.
37. B. Zhang, Y. Tian, J. Zhang and W. Cai, *Vacuum*, 85 (2011) 986.
38. S. N. Pusawale, P. R. Deshmukh and C. D. Lokhande, *Appl. Surf. Sci.*, 257 (2011) 9498.
39. F. Li, J. Song, H. Yang, S. Gan, Q. Zhang, D. Han, A. Ivaska and L. Niu, *Nanotechnology*, 20 (2009) 455602.
40. M. Kwoka, N. Waczyńska, P. Kościelniak, M. Sitarza and J. Szubera, *Thin Solid Films*, 520 (2011) 913.
41. M. Kwoka, L. Ottaviano, N. Waczyn'ska, S. Santucci and J. Szuber, *Appl. Surf. Sci.*, 256 (2010) 5771.
42. Y. F. Lee, K. Chang, C. Hu and K. Lin, *J. Mater. Chem.*, 20 (2010) 5682.

© 2017 The Authors. Published by ESG (www.electrochemsci.org). This article is an open access article distributed under the terms and conditions of the Creative Commons Attribution license (<http://creativecommons.org/licenses/by/4.0/>).